Morphology and scaling of impact craters in granular media

Amanda M. Walsh and John R. de Bruyn
Department of Physics and Physical Oceanography
Memorial University of Newfoundland
St. John's, Newfoundland, Canada A1B 3X7

We study the size and morphology of impact craters formed when a steel ball is dropped into a container of small glass beads. We find that both the depth (measured from the original surface) and diameter of the crater are proportional to the 1/4 power of energy. This is as expected if the energy of impact goes into excavating the crater and material strength is unimportant. We observe a variety of crater morphologies as a function of impact energy and grain size: simple craters, craters with a central peak, craters with slump terraces around the perimeter, and multi-ringed craters. The progression of these changes in morphology is similar to that observed in lunar craters.

Craters on the moon and planets form as a result of meteor impacts. Various crater morphologies are observed, with features such as central peaks, slump terraces, and multiple rings appearing as the crater size increases [1, 2]. Power-law scaling laws relating crater diameter w and the energy of impact E can be derived in certain limits [3]. If the kinetic energy of the projectile goes into excavating the crater against gravity one can show that $w \propto E^{1/4}$, while if the strength of the target material is important, $w \propto E^{1/3}$ [1, 3]. Craters formed by nuclear explosions follow an intermediate scaling, but gravity dominated scaling is expected to hold for large lunar craters. Laboratory studies of impact crater formation typically involve firing projectiles into a target at speeds of several kilometers per second [4], but experiments on crater formation in granular materials have also been reported [5–7].

We studied the formation of craters by dropping a steel ball into loosely packed glass beads. Balls with diameters 2.54 cm and 1.27 cm and masses 66.0 g and 8.35 g respectively were dropped into a large container of glass beads with diameters D_g ranging from 45-90 μm up to 300-425 μm. The beads were poured evenly into the experimental container prior to each run, with the two smallest sized beads being poured through a sieve. The surface was smoothed with a straight edge but otherwise the beads were used "as poured," with no shaking. The packing fraction of the beads ranged from 56% for the smallest beads up to 62% for the largest. The impact energy E is equal to mgh, where m is the mass of the ball and h is the release height. h was varied in the range 2 to 90 cm, corresponding to $10^5 \leq E \leq 6 \times 10^6$ ergs. In most cases, the steel ball was completely buried in the target material after the impact [8].

Figure 1 shows examples of the craters observed. At low energies and with large beads, simple bowl-shaped craters surrounded by a uniform rim are formed (Fig. 1(a)). For larger E or smaller D_g, a central peak appears (Fig. 1(b)). This peak is associated with the appearance of granular jets [9–11] which result from the inward rebound of displaced grains after passage of the projectile. At still higher energy and with the smallest beads, the craters have less well defined rims, flat bottoms, and terraces around the perimeter (Fig. 1(c)). The terraces result when the original crater walls are so steep that they collapse under gravity. Terracing was observed only for the smallest beads, and since the formation of terraces requires the granular medium to have some material strength, this indicates that these beads are slightly cohesive. At the highest energies studied, craters with multiple rings and a complex central morphology form. Figure 1(d) shows the range of E and D_g over which the different morphologies are observed. This sequence of crater morphologies is the same as that observed on the moon and elsewhere [1, 2].

We measured the crater diameter w at the top of the crater rim, as well as two versions of the crater depth: d, measured from the level of the original surface to the lowest point on the crater floor and the depth, and d_t, measured from the top of the rim to the crater floor. We non-dimensionalized our data by scaling distances by the bead diameter D_g and energy by the energy required to raise one bead a distance D_g against gravity. Fig. 2 is a log-log plot of the scaled crater width w' as a function of scaled energy E' for five different bead sizes and two ball diameters. The data for the four larger bead sizes are well described by a 1/4 power law over more than three orders of magnitude in scaled energy, as expected in the gravity-limited regime. The diameters of craters in the smallest beads (diamonds) fall significantly below the other data and show a weaker dependence on E'. This is mainly due to the fact that with the smallest beads, a significant fraction of the impact energy goes into the formation of large granular jets. This implies a smaller w for a given E for these beads, as observed, and in fact if *all* the energy goes into the jet, a simple argument predicts that $w =$ constant, consistent with the observed slow variation of w with E. These beads are also significantly influenced by air drag and cohesion, which likely arises due to atmospheric humidity.

The scaled crater depth d', measured from the original surface level to the lowest point in the crater, was also studied. The data sets for the different bead sizes are each well described by a 1/4 power law in E'. However, while

the power law *exponent* does not depend on D_g within our uncertainties, our scaling does not completely account for the effects of particle size here, and the data do not collapse onto a single line. Craters in smaller beads are slightly shallower than for larger beads, likely due to the increased effects of air drag and cohesion.

The rim-to-floor depth d_t differs from d due to the height of the crater rim and to compaction of the target material during impact. d_t is also well described by a power law with an exponent close to 1/4 at low E' but flattens out at higher energies, suggesting a change in the details of the crater formation process at high E'. As a result of this, the ratio w'/d'_t of crater diameter to rim-to-floor depth is constant and equal to 8.4 ± 0.4 at low E', in the regime where all crater dimensions scale as $E'^{1/4}$, but increases at higher E' as the behavior of d'_t changes. This ratio has been measured for lunar craters: it is approximately 5 for simple craters (i.e., low energies) but becomes larger for complex craters (high energies) [1]. Our low energy value is slightly higher than for lunar craters, probably due to differences in material properties, but the same trend is observed as E' is increased — craters formed in high energy impacts are relatively wider and flatter than low energy craters.

This research was supported by NSERC of Canada. We are grateful to P. Habdas and K. Holloway for their contributions to this work.

[1] H. J. Melosh, Impact Cratering: A Geologic Process (Oxford University Press, New York, 1989).
[2] H. J. Melosh and B. A. Ivanov, Annu. Rev. Earth Planet. Sci. **27**, 385 (1999).
[3] K. A. Holsapple, Annu. Rev. Earth Planet. Sci. **21**, 333 (1993).
[4] P. H. Schultz, Int. J. Impact Engng. **5**, 569 (1987).
[5] J. C. Amato and R. E. Williams, Am. J. Phys. **66**, 141 (1998).
[6] J. S. Uehara, M. A. Ambroso, R. P. Ojha, and D. J. Durian, Phys. Rev. Lett. **90**, 194301 (2003).
[7] A. M. Walsh, K. A. Holloway, P. Habdas, and J. R. de Bruyn, Phys. Rev. Lett. **91**, 104301 (2003).
[8] J. R. de Bruyn and A. Walsh, Phys. Rev. E, to be published.
[9] A. Walsh and J. R. de Bruyn, unpublished.
[10] S. T. Thoroddsen and A. Q. Shen, Phys. Fluids **13**, 4 (2001).
[11] R. Mikkelsen, M. Versluis, E. Koene, G.-W. Bruggert, D. van der Meer, K. van der Weele, and D. Lohse, Phys. Fluids **14**, S14 (2002).

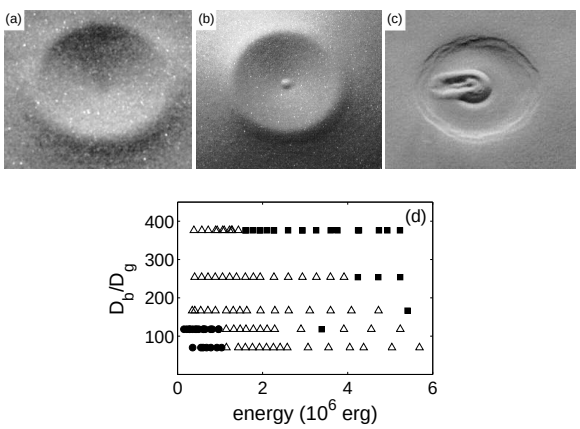

FIG. 1: Impact craters formed by dropping a 2.54 cm diameter, 66.0 g steel ball vertically into a container of small glass beads. (a) A simple crater formed in beads of diameter D_g = 180-250 μm when the ball was released from a height h of 14.8 cm. The rim-to-rim crater diameter w is 6.62 cm. (b) A crater with a small central peak and w = 8.08 cm. Here h = 32.5 cm and D_g = 180-250 μm. (c) A complex crater with w = 5.66 cm formed in beads with D_g = 45-90 μm for h = 40.1 cm. (d) The range of existence of the different crater morphologies in terms of the impact energy and the ratio of the ball diameter to the bead diameter, D_b/D_g. Circles: simple craters; triangles: craters with a central peak; squares: craters with multiple rings.

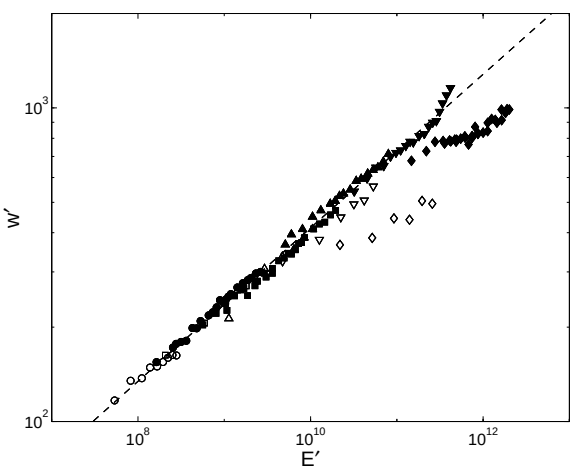

FIG. 2: The scaled crater diameter as a function of scaled energy. Solid symbols are for craters formed with a 2.54 cm diameter steel ball and open symbols for a 1.27 cm ball. The different symbols indicate different sized glass beads: diamonds, 45-90 μm, downward-pointing triangles, 75-125 μm, upward-pointing triangles, 125-180 μm, squares, 180-250 μm, and circles, 300-425 μm. The dashed line is a fit to the data for the four larger bead sizes and the large ball, and has a slope of 0.245 ± 0.002.